Microstructure-Mechanical Property Relationships in Isothermally Transformed Vanadium Steels

J. A. TODD and P. LI

The relationships between the interphase precipitation reaction and the mechanical properties of an Fe-0.2C-1.0V-0.5Mn steel were studied after isothermal transformation in the temperature range 600 °C to 750 °C. The strength and room temperature toughness of the transformed steel are found to be determined by the austenitization temperature, vanadium carbide solubility, volume fraction of VC available for precipitation, size of the precipitates, and ferrite grain size. Yield strength increments due to precipitation are predicted by Melander's model for critical resolved shear stress, when all the available carbide precipitated as interphase VC. For lower austenitization temperatures, yield strength increments are modeled by a bimodal distribution of undissolved and interphase (or matrix) precipitates. Six classifications of VC morphologies are identified in the transformed microstructures, but one of these, the "fibrous" VC morphology, could not be associated with degradation of toughness as suggested by Mishima. The impact transition temperatures are approximated by regression analyses for bainitic steels. The results show that both strength and toughness can be simultaneously optimized in this steel and suggest that microstructures with strength and toughness levels equivalent to those of quenched and tempered steels can be produced in vanadium steels by the *direct* decomposition of austenite.

I. INTRODUCTION

THE interphase precipitation reaction occurs in vanadium steels by the direct decomposition of austenite to ferrite with vanadium carbide, carbonitride, or nitride particles being precipitated at the austenite : ferrite interphase boundary during the transformation.[1-6] Planar sheets or curved boundary arrays of particles are observed by transmission electron microscopy[7,8] and are responsible for significantly increasing the yield strength of vanadium-microalloyed high strength low alloy (HSLA) steels.[9-13] However, the interphase precipitation strengthening has a deleterious effect on impact toughness levels, which is usually improved by grain refinement through, for example, normalizing or controlled rolling.[14-18]

Recent studies by Mishima[11,19] and Todd and Parker,[20] of isothermally transformed Fe-C-V alloys, have shown that when the VC interphase precipitate morphology is combined with a large prior austenite grain size (~200 μm for austenitizing temperature 1200 °C), high strength but extremely brittle microstructures result, regardless of the transformation temperature. However, for an austenitizing temperature of 1000 °C (ferrite grain size ~10 to 15 μm), a distinct difference was observed between samples transformed at temperatures above and below the nose of the ferrite C-curve. The above nose transformation products gave room temperature Charpy impact toughness values of 228 J compared to 3 J for microstructures developed at the lower temperatures. This extreme degradation in toughness level was attributed by Mishima[19] to the presence of a fibrous vanadium carbide morphology, and it was proposed that the elimination of this morphology would restore the high impact values.

According to Honeycombe,[5] precipitation of fibrous VC is rare (~5 pct total VC precipitate) in an isothermally transformed Fe-0.2C-1.0V steel, but Batte,[21] Edmonds,[22] and Law[23] have shown that additions of 1.5 pct Mn or 1.5 pct Ni can increase the fibrous morphology to ~20 pct of the total VC precipitate. The present study was undertaken to make a systematic study of the microstructures in an isothermally transformed Fe-0.2C-1.0V-0.5Mn steel and to investigate the role of the interphase and fibrous vanadium carbide morphologies in determining the strength and impact toughness levels of this steel.

J. A. TODD, Assistant Professor, and P. LI, Graduate Research Assistant, are with the Departments of Materials Science and Mechanical Engineering, University of Southern California, Los Angeles, CA 90089-0241.

Manuscript submitted July 15, 1985.

II. EXPERIMENTAL PROCEDURE

A. *Material*

The chemical composition (weight pct) of the steel used in this study was Fe-0.19C-1.14V-0.45Mn-0.001N. The alloy was prepared from high purity elements (99.9+ pct) and induction melted under argon in a magnesium oxide crucible. A 10 kg, 7 cm diameter ingot was cast in a copper mold in an argon atmosphere. The ingot was upset forged at 1200 °C in air and cross rolled to a rectangular section 7 cm wide by 1.5 cm thick.

B. *Dilatometry*

A Theta Dilatronic model IIIR dilatometer was used to determine isothermal transformation diagrams for the steel. Isothermal measurements were carried out in vacuum following austenitization at 1200 °C, 1000 °C, or 900 °C for 15 minutes. Cylindrical specimens (1 cm long, 0.5 cm outer diameter, and 0.3 cm internal diameter) were rapidly quenched to the isothermal transformation temperature by cold helium gas and maintained at that temperature until the transformation, as monitored by length changes, was complete.

C. *Heat Treatment*

Isothermal heat treatments of blanks (12 mm × 12 mm × 70 mm) for mechanical property and microstructural examination were carried out using a vertical

tube furnace with an argon atmosphere and a molten salt bath. Austenitization was performed at 1200 °C, 1000 °C, and 900 °C for 1 hour followed by a quench into a molten salt bath controlled to within ±5 °C. Samples were transformed for 4 to 6 minutes so that they were fully transformed to ferrite plus VC and were then quenched into water. Isothermal transformation temperatures were chosen to be above and below the nose of each ferrite C-curve and are given in Table I.

D. *Mechanical Properties*

Room temperature tensile tests were carried out using a 135 kN Houston United testing machine at a strain rate of 1.67×10^{-3} per second. Room temperature Charpy impact tests (LT orientation) were performed on a 325 J (240 ft-lb) capacity machine according to ASTM E-23-72 specifications.

E. *Microscopy*

Fracture surfaces of the Charpy test specimens were examined with a Cambridge S4-10 scanning electron microscope operated at 20 kV. Thin foils were prepared for transmission electron microscopy by cutting slices approximately 0.5 mm thick from the broken Charpy specimens and chemically thinning to approximately 0.15 mm using a solution of HF and H_2O_2. Discs, 3 mm in diameter, were punched and ground to 0.06 mm thickness, followed by jet polishing in Cr_2O_3-CH_3COOH solution. The foils were examined with a Philips 420T scanning transmission electron microscope operated at 120 kV.

III. RESULTS

A. *Transformation Characteristics*

The TTT diagrams for the 1200 °C, 1000 °C, and 900 °C austenitization treatments are compared in Figure 1. The ferrite nucleation rate is decreased and the temperature at the nose of the ferrite C-curve is reduced as the austenitization temperature decreases. Two competing effects contribute to these curves: (a) decreased ferrite grain size, due to undissolved carbides at 1000 °C and 900 °C, which increases the ferrite nucleation and growth kinetics and (b) lower solubility of VC at the 1000 °C and 900 °C austenitization temperatures leading to reduced hardenability. After 4 minutes at the isothermal transformation temperatures chosen, all samples were fully transformed to ferrite and vanadium carbide. Ferrite grain sizes, measured from the fully transformed microstructures, were 135 μm, 15 μm, and 10 μm for the 1200 °C, 1000 °C, and 900 °C austenitization treatments, respectively.

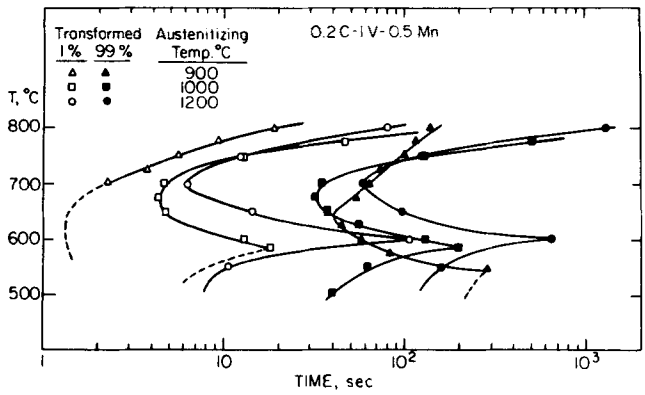

Fig. 1—Isothermal transformation diagrams of Fe-0.2C-1.1V-0.5Mn-0.001N steel austenitized at 1200 °C, 1000 °C, and 900 °C.

B. *Mechanical Properties*

The room temperature tensile and impact properties of samples isothermally transformed at temperatures above and below the nose of each ferrite C-curve are shown in Table I. For the 1200 °C austenitization treatment the yield stress increased from 836 MPa to a fracture stress of 1211 MPa (10 pct and 0 pct reduction in area, respectively) as the transformation temperature was lowered from 740 °C to 650 °C. Both the above and below nose microstructures were brittle having only 3 J room temperature Charpy impact energies. The poor toughness in these materials was attributed to the large prior austenite grain size (~250 μm). Isothermal transformation after the 1000 °C austenitization resulted in a marked difference between the 715 °C (above nose) and the 650 °C (below nose) impact toughness. Room temperature Charpy energies of 228 J and yield strengths of 575 MPa were observed at the higher transformation temperature, compared to Charpy energies of 5 J and yield strengths of 710 MPa at the lower transformation temperature. Such an increase in toughness could not have been predicted from the changes in ductility (81 pct to 68 pct RA; 26 pct to 16 pct elongation) or hardness measurements (R_c 30 to 33). These data confirm similar toughness variations observed by Mishima[19] for Fe-0.2C-1V-0.5Mn, Fe-0.2C-1V-0.5Mn-3Ni, and Fe-0.1C-0.5V-0.5Mn-3Ni steels austenitized at 1000 °C and isothermally transformed at temperatures above and below the ferrite C-curve nose for

Table I. Mechanical Property Data for Isothermally Transformed Steel

Austenitization		Transformation		σ_y	σ_{UTS}				CVN Room	Ferrite Grain
#	Temp., °C	Time (min)	Temp., °C	MPa	MPa	Pct RA	Pct ε	R_c	Temp., J	Size, μm
V1	1200	4	740*	836	1012	10	6	35	3	134
V2	1200	4	650	1211	1211	0	2	43	3	134
V3	1000	6	715*	575	715	81	26	30	228	15
V4	1000	6	650	710	800	68	16	33	5	15
V5	900	4	715*	357	598	77	25	24	325	10
V6	900	4	615	426	533	75	36	23	324	10

*above nose transformation

1 hour. In contrast, the samples austenitized at 900 °C and transformed at 715 °C and 615 °C were significantly lower in strength (357 MPa and 426 MPa yield strengths respectively), but both gave exceptionally high toughness values of 325 J. The ferrite grain size was 10 μm compared to 15 μm for samples transformed after 1000 °C austenitization.

C. *Microscopy*

Optical micrographs of the as-received and isothermally transformed microstructures are presented in Figures 2(a) through 2(d). All the microstructures were ferritic with those of the as-received and the 900 °C austenitization showing a texture in the rolling direction. Undissolved carbides were observed in the ferrite matrix (for the 1000 °C and 900 °C austenitization temperatures only) and were shown by SEM to increase in number as the austenitization temperature was reduced.

The fracture surfaces of the Charpy impact test specimens are shown in Figures 3(a) through 3(c). Cleavage failures were observed for samples austenitized at 1200 °C and isothermally transformed at 740 °C or 650 °C for 4 minutes (Figure 3(a)). When the austenitization temperature was reduced to 1000 °C, a mixed dimple rupture/quasi-cleavage fracture surface was observed for isothermal transformation at temperatures above the nose of the ferrite C-curve (Figure 3(b)), whereas cleavage fracture only was observed for the below nose transformation temperature (Figure 3(c)). For the 900 °C austenitization treatment, mixed dimpled rupture/quasi-cleavage fractures, similar to those of Figure 3(b), were observed for both transformation temperatures.

D. *Transmission Electron Microscopy*

The microstructures of the as-received steel were complex and contained three size ranges of vanadium carbide

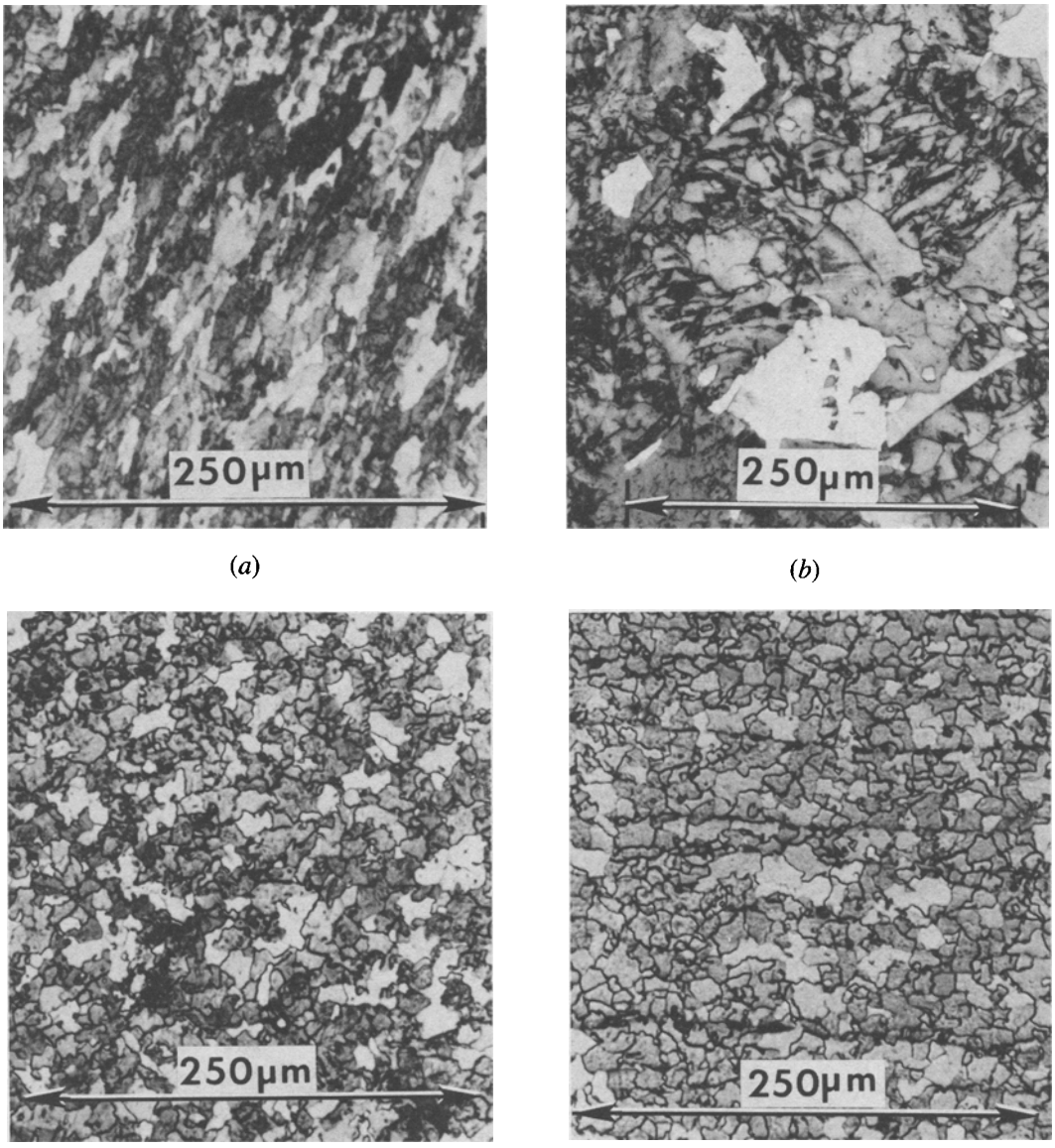

(*a*) (*b*) (*c*) (*d*)

Fig. 2—Optical micrographs of (*a*) as-received microstructure, (*b*) 1200 °C, 1 h; 650 °C, 4 min, (*c*) 1000 °C, 1 h; 715 °C, 6 min, and (*d*) 900 °C, 1 h; 715 °C, 4 min.

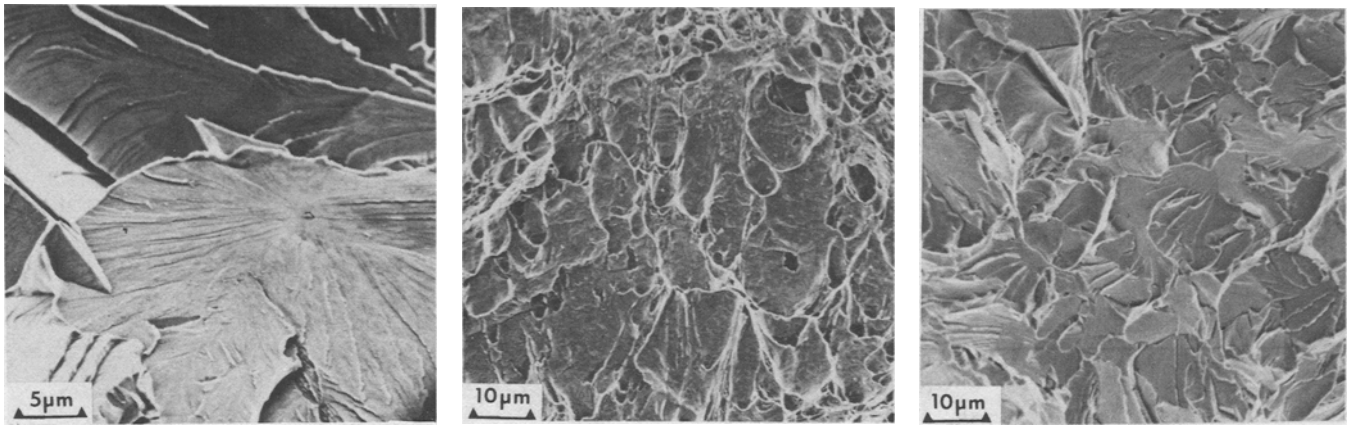

(a) (b) (c)

Fig. 3—Scanning electron micrographs of fracture surfaces: (*a*) 1200 °C, 1 h; 740 °C, 4 min, (*b*) 1000 °C, 1 h; 715 °C, 6 min, and (*c*) 1000 °C, 1 h; 650 °C, 6 min.

precipitates: large (~0.1 μm to 0.35 μm), intermediate (~1000 nm to 5000 nm), and fine (~400 nm to 2500 nm) particles. The large precipitates were distributed both within the grains and at the ferrite grain boundaries whereas the intermediate precipitates were often aligned in rows parallel to the rolling direction (Figure 4). The fine precipitates could be associated with both interphase precipitation and precipitation on dislocations. Occasional regions containing what appeared to be fibrous precipitates ~100 nm in length were observed.

1. *1200 °C austenitization*

Interphase vanadium carbide was the dominant precipitate in both the 740 °C and 650 °C isothermally transformed microstructures after austenitization for 1 hour at 1200 °C (Figure 5). Intersheet spacings of ~17 to 25 nm were measured for the 740 °C transformation decreasing to a range ~7 to 20 nm at 650 °C. Fibrous carbides, up to ~150 nm in length, were occasionally observed after transformation at 740 °C but have not been detected in the 650 °C microstructure. A ferrite region containing two orientations of fibrous carbides is shown in Figures 6(a) through 6(d). In addition to the closer intersheet spacings, a higher dislocation density was observed in the 650 °C microstructure. Both the 740 °C and, to a greater extent, the 650 °C microstructures contained coarser, VC precipitates, some with a faceted hexagonal morphology, which had precipitated in the austenite prior to the transformation to ferrite. The un-

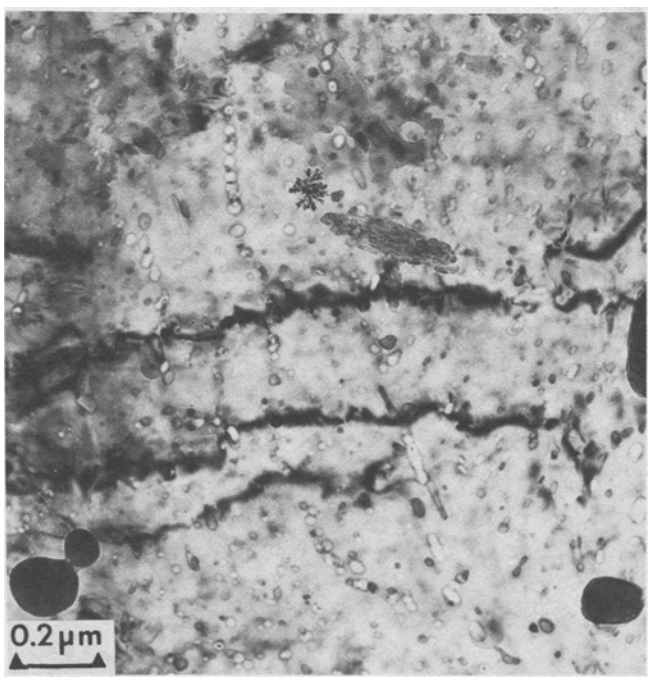

Fig. 4—Transmission electron micrograph of the as-received microstructure.

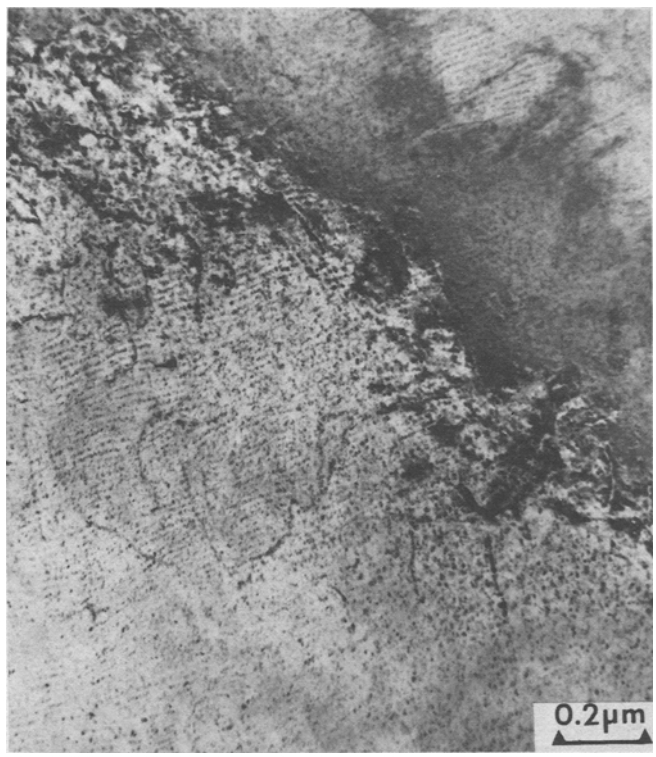

Fig. 5—Transmission electron micrograph of interphase precipitation. 1200 °C—1 h, 4 min 740 °C.

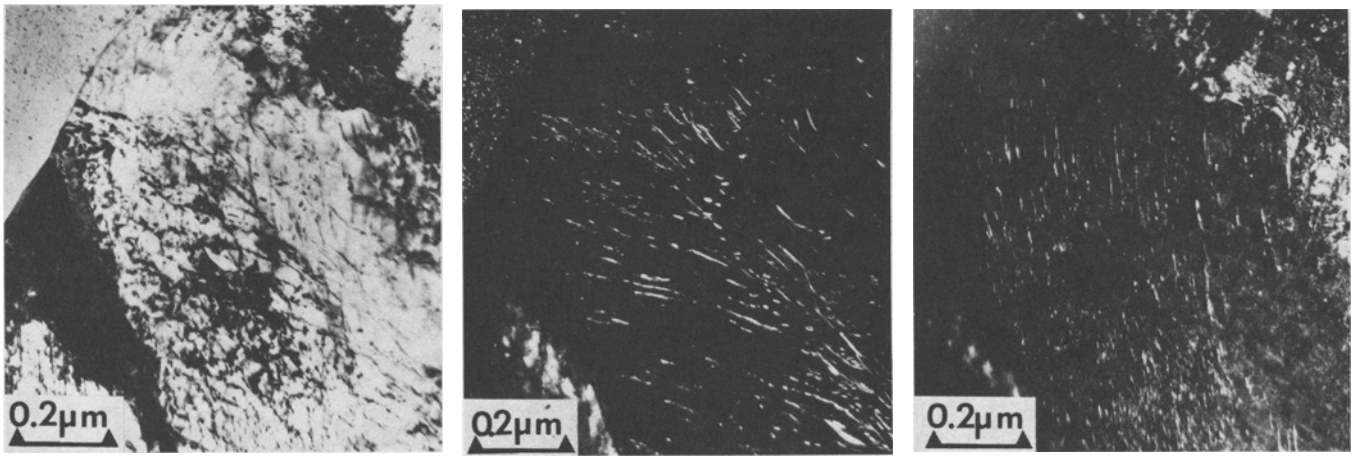

(*a*) (*b*) (*c*)

Fig. 6—Transmission electron micrographs of the fibrous carbide morphology. 1200 °C—1 h, 4 min 740 °C. (*a*) Bright field, (*b*) dark field showing first orientation of fibers, and (*c*) dark field showing second orientation of fibers.

dissolved carbide was distinguished from the VC precipitation in austenite by direct quenching experiments from 1200 °C, 1000 °C, and 900 °C. The interphase precipitate was either absent from these regions or the inter-row spacing increased. Figure 7 shows the interphase precipitate row spacing increasing from left to right toward a region containing only VC precipitates formed in the austenite (arrow). These larger carbides will be referred to as VC precipitation in austenite.

2. *1000 °C austenitization*

After austenitization at 1000 °C and isothermal transformation at 715 °C and 650 °C, much more complex microstructures developed. Undissolved carbides, up to 0.35 μm in size and surrounded by precipitate free zones, were observed pinning the prior austenite grain boundaries and also within the ferrite matrix (Figure 8(a)). The ferrite grain size was 15 μm.

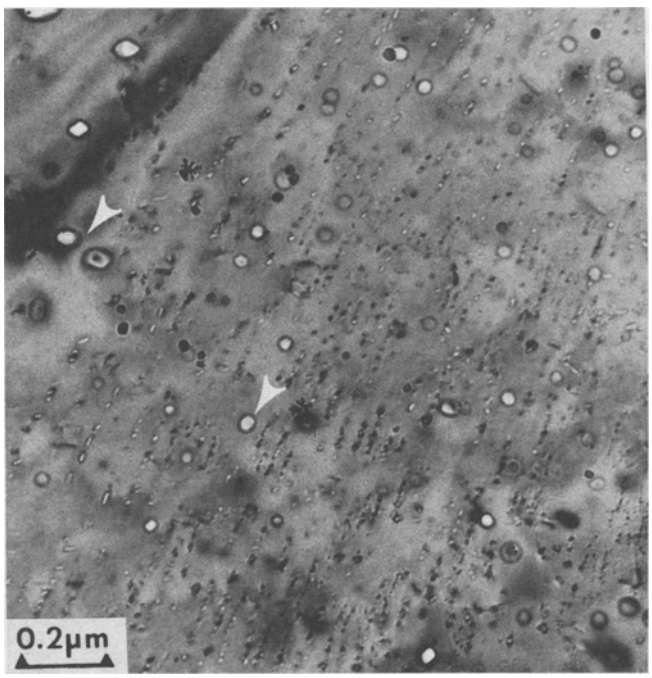

Fig. 7—Transmission electron micrograph of interphase precipitation and VC precipitated from austenite (arrows). 1200 °C—1 h, 4 min 650 °C.

The 715 °C microstructure contained two types of precipitate sheets with spacings varying from ~23 to 85 nm. The first (Figure 8(a)), unlike interphase precipitation, was not restricted to one variant of vanadium carbide and may be associated with the rows of precipitates (aligned or interphase) observed in the as-received microstructure. The second type was sheets of interphase precipitate, which also contained fibrous vanadium carbides up to 0.13 μm in length and 0.013 μm wide. Bright- and dark-field micrographs of the interphase precipitate are shown for clarity in Figures 8(c) and 8(d). Some of these fibers had an "S-shape" (arrows) rather than unidirectional appearance (Figure 8(c)). Longer fibers, up to 0.4 μm in length and 0.013 μm wide, were observed adjacent to precipitate free zones at the ferrite grain boundaries (Figure 8(b)).

After 6 minutes at the below nose transformation temperature, interphase precipitation with a sheet spacing of ~17 to 30 nm was observed (Figure 8(e)). Fibers (~0.2 μm long, 6 nm wide) were occasionally observed (Figure 8(f)), possibly associated with dislocations produced during the austenite to ferrite phase transformation. These fibers could be clearly identified by dark-field imaging. Higher dislocation densities were developed at the lower transformation temperature. In addition to the interphase precipitation, precipitation from supersaturated ferrite, referred to as matrix precipitation, was found to occur either later during the transformation or on cooling to room temperature. Ferrite grains containing three orthogonal variants of VC platelets (~7 to 30 nm) were observed in such regions, predominantly for the 650 °C transformation temperature.

3. *900 °C austenitization*

Undissolved carbides dominated the microstructures of the 715 °C and 615 °C isothermally transformed samples after austenitization for one hour at 900 °C (Figure 9(a)). Short fibers (~7 to 100 nm in length and ~3 to 10 nm wide) have been observed in the above nose microstructure (Figure 9(b)), and regions of interphase precipitation, which occur nonuniformly throughout the ferrite grains, were identified in both the 715 °C and the 615 °C microstructures.

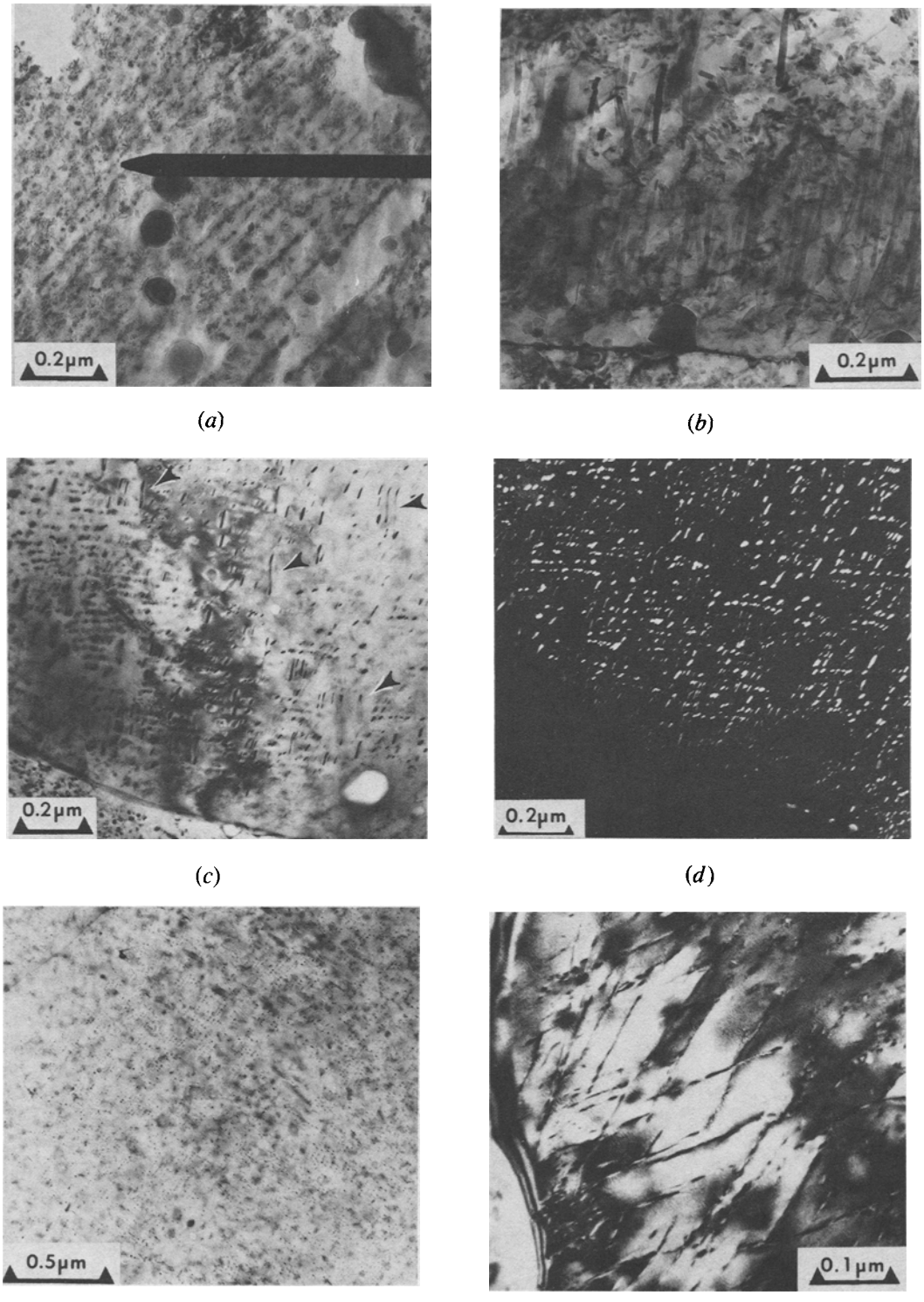

Fig. 8—Transmission electron micrographs of samples austenitized at 1000 °C. (*a*) 6 min 715 °C—undissolved carbides, precipitate free zones and row precipitates. (*b*) 6 min 715 °C—long fibers (0.4 μm) associated with precipitate free zones at grain boundaries. (*c*) 6 min 715 °C—bright field showing interphase and fibrous precipitates (arrows). (*d*) 6 min 715 °C—dark field of (c). (*e*) 6 min 650 °C—interphase precipitation. (*f*) 6 min 650 °C—fibers precipitated on dislocations.

IV. DISCUSSION

The transmission electron microscopy (TEM) studies have identified the following six classifications of vanadium carbide morphologies in the isothermally transformed steel:

1. Undissolved carbides
2. Precipitation in austenite
3. Interphase precipitation
4. "Fibrous" morphology
5. Matrix precipitation
6. Precipitation on dislocations.

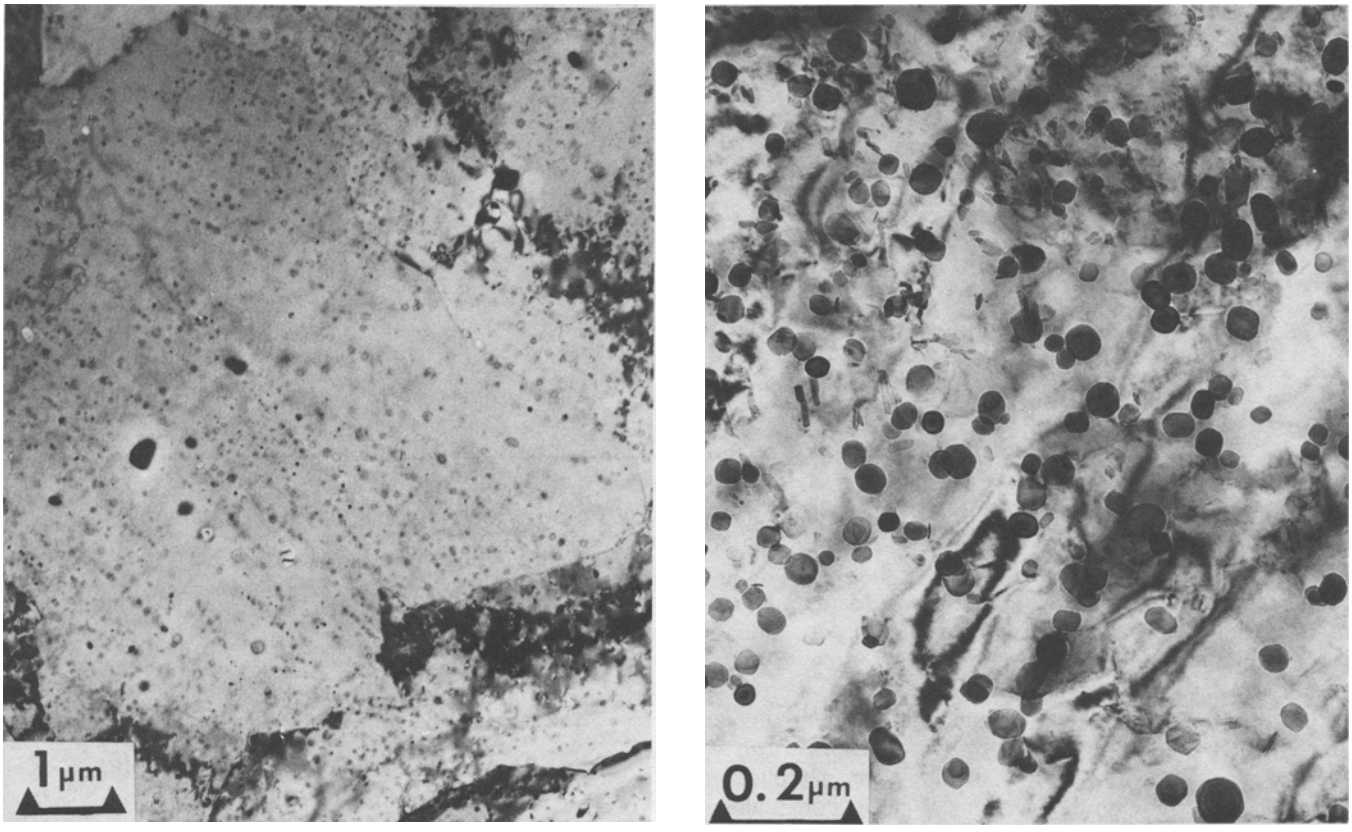

(*a*) (*b*)

Fig. 9—Transmission electron micrographs of samples austenitized at 900 °C. (*a*) 4 min 615 °C—undissolved carbides within grains and at grain boundaries. (*b*) 4 min 615 °C—undissolved carbides and "short fibers".

The "fibrous" category includes the long fibers (up to 0.4 μm); short fibers (<0.1 μm); "S-shaped" precipitates; and "effective fibers" produced by either coalescence of interphase precipitates along the rows or by coarsening of precipitates along dislocation lines. The fibrous morphology was observed predominantly at the higher transformation temperatures and to the greatest extent after 1000 °C austenitization. However, since the microstructures transformed at 715 °C contained the greatest number of fibers (but still <5 pct) and gave high room temperature Charpy toughness values, it is concluded that, at low volume fractions, the fibrous morphology was not detrimental to toughness.

Matrix precipitation was observed only in samples transformed at the below nose temperatures. Interphase precipitation was observed for all temperatures throughout the transformation range. The TEM studies clearly showed that the interphase and matrix vanadium carbides were the precipitates making the greatest contributions to the strength of this steel.

A. *Solubility Calculations*

In order to determine the strengthening effect of the vanadium carbide precipitates, calculations of the amount of VC available for precipitation at each austenitizing temperature have been made using solubility product data[24,25,26] and applying the methods developed by Wadsworth, Keown, and Woodhead.[27,28,29] The solubilities of the carbide in both austenite and ferrite may be expressed by the solubility product relationship, which may be written, for a compound AB_n as:

$$\ln [A][B]^n = P - Q/T \qquad [1]$$

where P and Q are constants and T is the absolute temperature.

The constants P and Q are given in Table II for vanadium carbide stoichiometries assumed to be $VC_{0.75}$ and VC. Data by Bungardt[25] were used for calculations of VC solubility in austenite, as they apply to steels with higher vanadium contents (up to 2 wt pct), and by Sekine *et al.*[30] for precipitation in ferrite. Calculations were made for an actual steel composition of Fe-0.19C-1.14V and have been made assuming the solubility product data could apply to both the carbides VC and $VC_{0.75}$, which represent the upper and lower bounds for the carbide VC_{1-x}.

The results are presented in Table III and show that for the 1200 °C austenitization, all the vanadium carbide will go into solution and be available for precipitation during

Table II. Solubility Data

	P	*Q*
$VC_{0.75}$ in austenite[25]	11.33	17660
$VC_{0.75}$ in ferrite[30]	13.02	21500
VC in austenite[31]	15.48	21897
VC in ferrite (best line from Refs. 30, 32, 33)	10.48	19115

Table III. Solubility Calculations VC and $VC_{0.75}$ in Austenite

T °C	K[Wt Pct]^2	Pct VC Undissolved	Pct VC for pptn	Pct $VC_{0.75}$ Undissolved	Pct $VC_{0.75}$ for pptn
1200	5.17×10^{-1}	0.00	100.00	0.00	100.00
1000	7.87×10^{-2}	46.05	53.95	57.90	42.10
900	2.41×10^{-2}	75.84	24.16	79.40	20.26
740	2.24×10^{-3}	96.70	3.30	96.63	3.37
715	1.44×10^{-3}	97.82	2.18	97.74	2.26
650	4.08×10^{-4}	99.36	0.64	99.44	0.56
615	1.92×10^{-4}	99.70	0.30	99.79	0.22
		VC and $VC_{0.75}$ in Ferrite			
740	2.74×10^{-4}	99.60	0.40	99.64	0.36
715	1.60×10^{-4}	99.75	0.25	99.82	0.18
650	3.45×10^{-5}	99.95	0.05	99.98	0.02
615	1.38×10^{-5}	99.98	0.02	100.00	0.00

isothermal transformation. For the 1000 °C austenitization, ~46 to 58 pct VC remains undissolved in the austenite with ~42 to 54 pct available for precipitation (depending on carbide stoichiometry) compared to ~75 to 80 pct undissolved carbide with ~20 to 25 pct available for precipitation at the 900 °C austenitization temperature. A significantly greater strengthening effect can, therefore, be achieved in fine grained ferrite after austenitizing at 1000 °C than at 900 °C. As shown by Wadsworth *et al.*,[28] the amount of vanadium carbide available for precipitation depends critically upon the elements V and C being added in the stoichiometric ratio for the compound they form. Assuming they formed the precipitate $VC_{0.75}$, the deviation from stoichiometry $r = -0.0095$ (*i.e.*, composition is slightly vanadium rich) was very small indicating that the maximum amount of carbide was available for precipitation. (The parameter r is a measure of the deviation from stoichiometry, given by $r = (pB_T - qA_T)$, where p, q, are the mass fractions of A and B in AB_n and A_T, B_T are the percentages of A and B in the alloy.) However, if the precipitating carbide had the stoichiometry VC, a larger deviation, $r = -0.06$, was calculated indicating that an adjustment of alloy composition would be necessary to gain maximum strengthening by VC precipitation. (N.B. The vanadium carbide precipitate has been referred to as VC throughout this study as the actual carbide stoichiometry VC_{1-x} is thought to be closer to VC than $VC_{0.75}$. It is not possible to distinguish these stoichiometries from the electron diffraction pattern analyses. The nitrogen level of the steel is so low (0.001 wt pct) that the precipitate is assumed to be closer to VC than VCN.) The solubility of VC in austenite decreases to ~0.3 to 3.3 pct as the temperature is lowered to the range 615 °C to 740 °C, consistent with the observed precipitation of VC in austenite (Figure 8).

B. *The Strengthening Effect of VC Precipitation*

A modified version of the Hall-Petch theory of yielding has been used to estimate the contribution of vanadium carbide precipitation and dislocation substructure to the yield strength of the isothermally transformed alloys.[9]

$$\sigma_y = \Delta\sigma_0 + \Delta\sigma_s + \Delta\sigma_g + \Delta\sigma_i \qquad [2]$$

where σ_y is the measured yield strength.

$\Delta\sigma_0$ = ferrite lattice friction stress[34] = 65 MPa

$\Delta\sigma_s$ = solid solution strengthening[35] = (32.5 × pct Mn) + (84 × pct Si) = 14.6 MPa (pct Si = 0)

$\Delta\sigma_g$ = ferrite grain size strengthening[9,35,36] = $k \times d^{-1/2}$; k = 17.9 Nmm$^{-3/2}$

$\Delta\sigma_i$ = strengthening from precipitation and dislocation substructure.

The results of these calculations are presented in Table IV and Figure 10.

For the 1200 °C austenitization treatment the strengthening effect of the vanadium carbide precipitate is estimated to be 707 MPa and 1082 MPa for the 740 °C and 650 °C transformations, respectively. The strengthening decreases to 349 MPa (above nose) and 484 MPa (below nose) after 1000 °C austenitization, compared to 106 MPa (above nose) and 175 MPa (below nose) for the 900 °C austenitization. At 900 °C the ferrite grain size makes an equal or greater contribution to the strength than the vanadium carbide precipitate.

The increase in yield strength due to dispersion strengthening by the vanadium carbide precipitates has been evaluated using a theory developed by Melander[37] for the critical resolved shear stress (CRSS) due to a distribution of impenetrable particles. Melander's calculation for CRSS was based on the statistical theory due to Hanson and Morris[38]

Table IV. Strengthening Due to VC Precipitation

Sample	σ_y, MPa Experimental	$\Delta\sigma_0$, MPa Calculated	$\Delta\sigma_s$, MPa Calculated	$\Delta\sigma_g$, MPa Calculated	$\Delta\sigma_i$, MPa Estimated
V1	836	65	15	49	707
V2	1211	65	15	49	1082
V3	575	65	15	146	349
V4	710	65	15	146	484
V5	357	65	15	171	106
V6	426	65	15	171	175

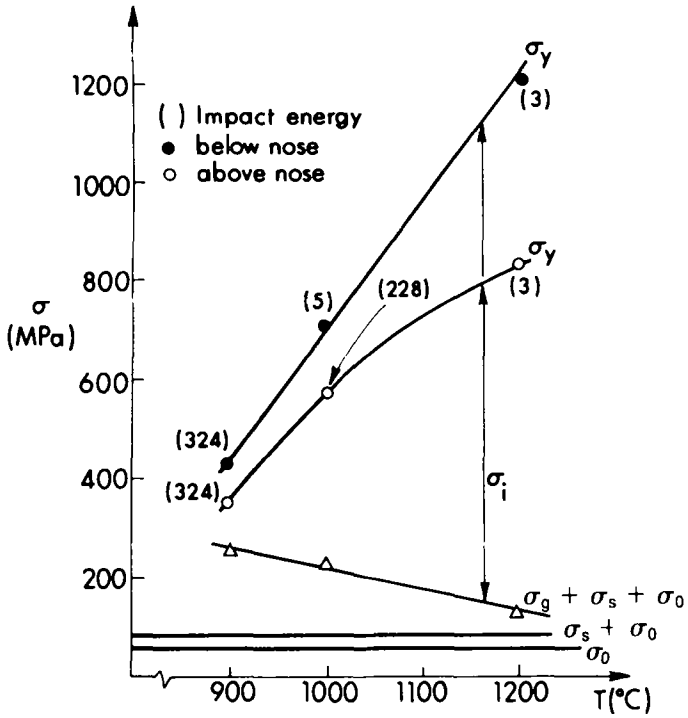

Fig. 10—Yield strength increments due to precipitation plotted as a function of austenitizing temperature.

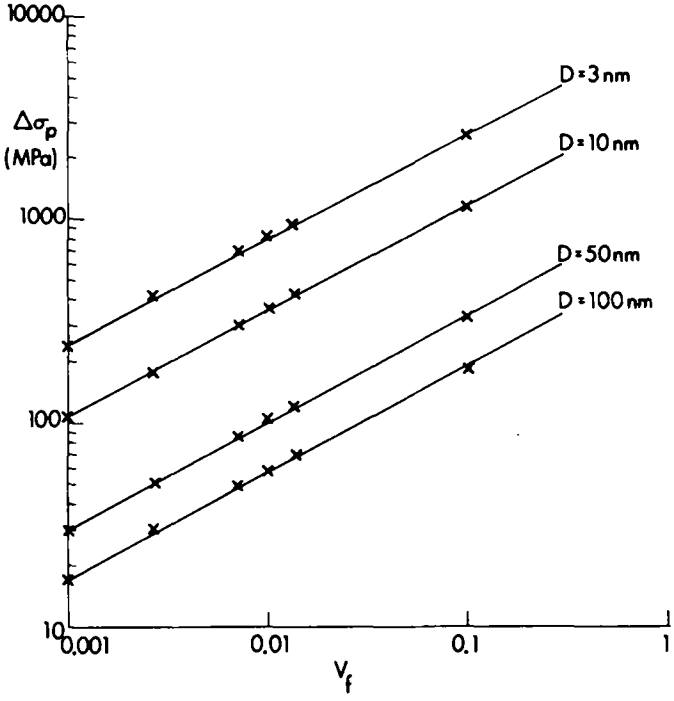

Fig. 11—Yield strength increments due to precipitation calculated from Melander's model for CRSS plotted as a function of volume fraction of carbide. x = calculated points.

and used an expression due to Bacon, Kocks, and Scattergood[39] for the Orowan strength. By comparison of the computed dispersion strengthening expected from a random array of obstacles of various strengths with experimental values of CRSS, determined by Ebeling and Ashby[40] for copper alloys containing silica particles, Melander derived the following relationship:

$$\Delta\sigma_y = 2\Delta\tau_y = \frac{3.56Gb}{4\pi l_r}\left(\frac{1+\nu-3\nu/2}{1-\nu}\right) \ln\left(\frac{l_r}{b}\right)\left[\frac{\ln\left(\frac{2D_g l_r}{b(D_g+l_r)}\right)}{\ln\left(\frac{l_r}{b}\right)}\right]^{3/2} \quad [3]$$

where G = shear modulus for ferrite = 8.03×10^4 MPa
ν = Poisson's ratio for ferrite = 0.33
b = dislocation Burgers vector = 0.25 nm
l_r = average distance between obstacle centers in the glide plane
D_g = geometric mean particle diameter evaluated from an extraction replica (Ashby and Ebeling[41])

In the present case it is assumed that the vanadium carbide precipitates are spherical and that $l_r = [(V/D_g \cdot V_f)]^{1/2}$, where V = mean volume per particle and V_f = volume fraction of particles. For a constant particle size, $D_g = D$, and $l_r = [(\pi \cdot D^2)/6V_f]^{1/2}$. The values of the yield strength increment, $\Delta\sigma_y$, due to dispersion strengthening calculated from the above equation are plotted in Figure 11 for volume fractions in the range 10^{-1} to 10^{-3}.

From the solubility calculations, the volume fractions of VC available for precipitation at 1200 °C, 1000 °C, and 900 °C have been calculated as 0.0136, 0.0073, and 0.0033, respectively. Mean particle sizes and interphase precipitate row spacings were determined from transmission electron micrographs and are presented in Table V. Using particle sizes of 5 nm (above nose) and 3 nm (below nose) and a volume fraction of 0.0136, Melander's equation predicts yield strength increments of 693 MPa (above nose) and 966 MPa (below nose) for the 1200 °C austenitization treatment. These values agree well with the experimentally determined values of 707 MPa and 1082 MPa for the samples transformed isothermally at 740 °C and 650 °C, respectively.

Although the interphase precipitate distribution is not random, replacement of the interparticle spacing, l_r, with the observed intersheet spacings overestimates the yield strength increments as 1091 MPa (above nose) and 1300 MPa (below nose) for the 1200 °C austenitization temperature. Such an approximation may be appropriate if the intersheet spacing, l_s, and the particle spacings within the sheets, l, are similar, but if $l \ll l_s$, the precipitates within the sheets will be strength determining. The present results suggest that in view of the difficulties in measuring l_s and l, the assumption of a random particle distribution predicts the experimentally observed yield strength increments well.

For the 1000 °C austenitization treatments, the yield strength increments due to both the interphase precipitate distribution (V_f = 0.0073) and the undissolved carbide distribution (V_f = 0.0033) have been calculated. When added, these values again predict well the experimentally observed strength increments (Table V). However, the additive effect of undissolved and interphase precipitates overestimates the strength increments for the 900 °C austenitization temperature. This can be attributed to the nonuniform nature of the interphase precipitation and the precipitation of VC on the undissolved carbides rather than by interphase or matrix precipitation during isothermal transformation.

Table V. Yield Strength Increments Due to Precipitation

Sample	V_f	Particle Size, nm	Particle Spacing, nm	$\Delta\sigma_y$ Experimental MPa	$\Delta\sigma_{(M)}$ Interphase MPa	$\Delta\sigma_{(M)}$ Undissolved MPa	$\Delta\sigma_y$ Total MPa	$\Delta\sigma_y$ Gladman MPa	ITT °C
V1	0.0136	5	20	707	693		693	412	155
V2	0.0136	3	14	1082	966		966	570	253
V3	0.0073	14	33	349	237		319		
V3	0.0063	35		349		82	319	211	0
V4	0.0073	6	22	484	439		521		
V4	0.0063	35		484		82	521	333	35
V5	0.0033	20		106	119		244		
V5	0.0103	40		106		125	244	150	−79
V6	0.0033	20		175	119		244		
V6	0.0103	40		175	119	125	244	150	−61

(M) = Melander's model

In view of the assumption of random, spherical precipitates and also the assumption that the fibrous morphology does not contribute significantly to the strength, the above model accounts for the experimental data extremely well. Similar calculations by Gladman *et al.*,[42] based on the Ashby-Orowan model of precipitation strengthening and the random-particle distribution model of Kocks[43] considerably underestimate the yield strength increments for the vanadium steel as shown in Table V. These results were calculated using the expression:

$$\Delta\sigma = \frac{5.9V_f^{1/2}}{X} \ln\left(\frac{X}{4.05 \times 10^{-4}}\right) \quad [4]$$

where X is the mean planar-intercept diameter of a precipitate in μm. The strengthening effects of the interphase and the undissolved carbides were added for the 1000 °C and 900 °C austenitization treatments.

The present results suggest that the theory for the critical resolved shear stress, proposed by Melander,[37] adequately predicts the strengthening effects of both an interphase precipitate distribution (1200 °C austenitization) and a bimodal distribution of undissolved and interphase precipitates (1000 °C austenitization).

C. *Evaluation of Toughness*

The wide variation in Charpy impact toughness levels observed in the isothermally transformed samples can be expressed in terms of an embrittlement vector which combines the competing effects of grain size refinement to increase toughness, and VC precipitation to reduce toughness. The regression equation for the Charpy impact transition temperature of bainitic steels is:[42,44]

$$\text{ITT (°C)} = -19 + 44(\text{pct Si}) + 700(\text{pct N}_{\text{free}})^{1/2} + 0.26(\sigma_D + \Delta_P + \Delta) - 11.5(d^{-1/2}) \quad [5]$$

where pct N_{free} (*i.e.*, pct N in solution) is estimated to be 0.001 pct

σ_D = Ashby-Orowan strengthening from dispersed second phase particles (MPa)

Δ_P = assumed strengthening contribution from random forest dislocations

Δ = contribution of dislocations in low angle grain boundaries

d = grain size (mm)

In the present study, $(\sigma_d + \Delta_P + \Delta)$ can be equated to $\Delta\sigma_i$.

The impact transition temperatures calculated from this expression are given in Table V, and impact curves incorporating the experimental room temperature toughness values and the calculated transition temperatures are sketched in Figure 12. It should be noted that the low nitrogen content (0.001 pct) of this steel is expected to be incorporated into the carbide as VCN. If the impact transition temperature calculations were made assuming there is no free nitrogen, all the curves are shifted 22 °C lower in transition temperature (here assumed to be the 54 J = 40 ft-lb transition temperature).

The results clearly show the transition from upper shelf to lower shelf toughness levels in the above and below nose microstructures produced after 1000 °C austenitization. From analyses of much experimental data, Gladman *et al.*[42,44] deduced that the impact transition temperature of polygonal-ferritic HSLA steels increased by 0.2 °C to 0.6 °C for each 1 MPa of strength increment. Thus, if the yield strength is increased by a known amount, the grain

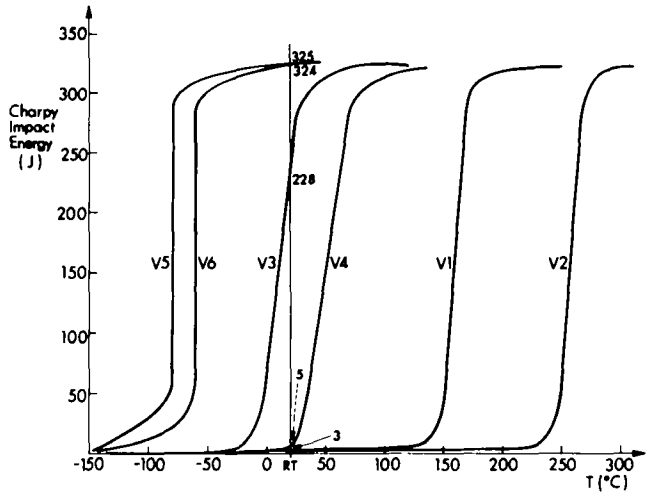

Fig. 12—Schematic diagram of impact transition temperatures determined by regression analysis.

size can be reduced accordingly to maintain the same toughness. For polygonal-ferritic steels, the smallest grain size readily attainable is ~4 μm. An upper limit to the precipitation strengthening contribution to the yield stress of ~300 MPa can be defined for this grain size if the impact properties are to remain unaffected. This limit is close to the yield strength increment of 349 MPa observed for the 1000 °C above nose isothermally transformed microstructure. When the precipitation strengthening is increased to 484 MPa (1000 °C, below nose), the room temperature toughness drops to the lower shelf value.

The strength and toughness values determined for the Fe-0.2C-1.0V-0.5Mn-0.001N steel suggest that maximum interphase precipitation strengthening combined with high toughness levels can be achieved in a steel with 0.0073 volume fraction of VC precipitate. This volume fraction corresponds to a composition in the range Fe-0.1C-0.5V-0.5Mn and would eliminate the large volume fraction of undissolved carbides, which give a much lower contribution to strength. However, data collected by Mishima[19] for this steel, after austenitization at 1000 °C and isothermal transformation for 1 hour, gave microstructures with 349 MPa yield strength and 18 J room temperature Charpy toughness for the above nose (750 °C) transformation product, and 413 MPa yield strength, 6 J impact toughness for the below nose (650 °C) transformation product. The lower above nose strength and toughness values can be associated with grain growth at the austenitization temperature resulting in a ferrite grain size ~40 μm and the longer isothermal transformation time allowing coarsening of the interphase precipitate. It is clear that the presence of undissolved carbides is essential for grain size refinement and the improvement of the toughness of these steels.

The precipitation of vanadium carbide in microalloyed, HSLA, and pressure vessel steels is generally associated with high strength and poor toughness levels. For example, Smith[45] has shown that secondary hardening of an Fe-0.23C-1V-1Mn gives a yield strength of ~1378 MPa (200 ksi) and hardness ~450 Vickers when tempered for 2 hours at 600 °C. The results obtained in the present work indicate that it is possible, by isothermal transformation, to produce yield strengths ~575 MPa (~83 ksi) with room temperature toughness values of 228 J. Such strength and toughness levels are consistent with specifications for quenched and tempered pressure vessel steels: *e.g.*, A533B Class 2, 485 MPa σ_y, 620 to 795 MPa σ_{UTS}: A542 Class 3, 515 MPa σ_y, 655 to 795 MPa σ_{UTS} and A543 Class 3, 485 MPa σ_y, 620 to 795 MPa σ_{UTS}. Typical toughness requirements might be 54 J at −40 °C. Our results suggest that microstructures with strength and toughness levels equivalent to those of quenched and tempered steels can be produced in vanadium steels by the *direct* decomposition of austenite.

V. CONCLUSIONS

1. The strength and toughness of isothermally transformed Fe-0.2C-1.0V-0.5Mn-0.001N steel is determined by the austenitization temperature, the solubility of vanadium carbide, the size and interparticle spacing of the VC precipitate, and the ferrite grain size of the transformed microstructure.
2. The maximum strengthening effect of vanadium carbide is achieved when the elements vanadium and carbon are added in the stoichiometric ratio.
3. The interphase precipitation reaction conveys maximum strength for the 1200 °C austenitization, but the resultant coarse grained microstructures have very poor room temperature Charpy impact toughness levels.
4. The yield strength increment due to the interphase precipitate strengthening (1200 °C austenitization) is predicted well by Melander's theory for the critical resolved shear stress.
5. For the 1000 °C austenitization treatment the yield strength increments are best modeled by the additive effects of both interphase and undissolved carbides.
6. The marked difference between the above and below nose toughness levels can be explained by regression analyses for bainitic steels incorporating the competing effects of precipitation strengthening and grain size refinement.
7. Six classifications of VC morphology have been identified in the Fe-0.2C-1.0V-0.5Mn-0.001N steel.
8. The fibrous vanadium carbide morphology observed in the above nose microstructures could not be associated with low values of the Charpy impact toughness.
9. The embrittling effects of grain boundary carbides appeared to be minor.
10. The greatest contribution to precipitation strengthening was made by the interphase and matrix vanadium carbide precipitates.
11. The 900 °C austenitization treatment gave the lowest strength levels but highest toughness values due to the fine ferrite grain size, undissolved carbides, and lower matrix strength.

ACKNOWLEDGMENTS

This work was performed with the support of an Engineering Foundation Research Award, AIME, 1983-1984, the University of Southern California Faculty and Research Innovation Fund, and the Vanadium International Technical Committee VANITEC, 1984-1985. The authors would like to thank Dr. A. M. Sage, Director, Vanitec, Mr. M. Korchinsky, Union Carbide Corporation, and Dr. E. R. Parker, U. C. Berkeley, for their helpful discussions in the preparation of this paper.

REFERENCES

1. A. T. Davenport, F. G. Berry, and R. W. K. Honeycombe: *Metal Sci. J.*, 1968, vol. 2, pp. 104-06.
2. A. D. Batte: Ph.D. Dissertation, Cambridge University, 1970.
3. R. W. K. Honeycombe: *Metall. Trans. A*, 1976, vol. 7A, pp. 915-36.
4. R. W. K. Honeycombe: *Met. Sci.*, 1980, vol. 14, pp. 201-14.
5. R. W. K. Honeycombe: *Proc. AIME Symposium*, Philadelphia, PA, Oct. 1983.
6. J. H. Woodhead: Proc. Seminar "Vanadium in High Strength Steels", Vanitec, Chicago, IL, 1979, pp. A-1.
7. A. T. Davenport and R. W. K. Honeycombe: *Proc. Roy. Soc.*, 1971, vol. 322, 1549, pp. 191-205.
8. R. A. Ricks and P. R. Howell: *Acta Metall.*, 1983, vol. 31, 6, pp. 853-61.
9. A. M. Sage, D. M. Hayes, C. C. Earley, and E. A. Almond: *Metals Technology*, 1976, vol. 19, 7, pp. 293-302.
10. P. R. Wilyman and R. W. K. Honeycombe: *Metal Science*, 1982, vol. 16, 6, pp. 295-303.

11. Y. Mishima, R. M. Horn, V. F. Zackay, and E. R. Parker: *Metall. Trans. A*, 1980, vol. 11A, pp. 431-40.
12. J. B. Benson: *Metal Science*, 1979, vol. 13, 6, pp. 366-72.
13. W. Roberts, A. Sandberg, and T. Siwecki: Proc. Vanitec Seminar on Vanadium Steels, Krakow, 8-10 Oct. 1980, pp. D1-D12.
14. J. M. Chilton and M. J. Roberts: *Metall. Trans. A*, 1980, vol. 11A, pp. 1711-21.
15. R. K. Amin, M. Korchinsky, and F. B. Pickering: *Metals Technology*, 1981, vol. 24, 7, p. 250.
16. G. Glover, R. B. Oldland, and R. Louis: Proc. HSLA Conference, Wollongong, NSW, Australia, Aug. 20-24, 1984.
17. "The Influence of Precipitation Mode and State of Ferrite on the Impact Properties of Vanadium Treated Steels" (BSC) V7: British Steel Corporation Final Report to Vanitec, Winterton House, Westerham, Kent TN16 1AJ, England, March 1984.
18. "The Effect of Additions of 0.15% to 0.45% Vanadium on the Microstructures of Laboratory Melts of an 0.06%C, 1.9%Mn Steel Plate Cooled Under Conditions Simulating those of a Coil": Vanitec Report DR 3/81, revised Feb. 1982, Winterton House, Westerham, Kent TN16 1AJ, England.
19. Y. Mishima: Ph.D. Dissertation, U. C. Berkeley, Berkeley, CA, Aug. 1979.
20. J. A. Todd and E. R. Parker: *Proc. Seventh Annual Conference on Materials for Coal Conversion and Utilization*, NBS, Gaithersburg, MD, Nov. 16-19, 1982, pp. 387-99.
21. A. D. Batte and R. W. K. Honeycombe: *J.I.S.I.*, 1973, vol. 211, pp. 284-89.
22. D. V. Edmonds: *J.I.S.I.*, 1972, vol. 210, 5, pp. 363-65.
23. N. C. Law: Ph.D. Dissertation, University of Cambridge, 1977.
24. B. Aronsson: Proc. AMAX Symposium "Steel-Strengthening Mechanisms", Zurich, Switzerland, 5-6 May, 1969, pp. 77-87.
25. K. Bungardt, K. Kind, and W. Oelson: *Arch. Eisenhüttenwes.*, 1956, vol. 17, pp. 61-66.
26. M. G. Fronberg and H. Graf: *Stahl u. Eisen*, 1960, vol. 80, pp. 539-41.
27. J. Wadsworth, S. R. Keown, and J. H. Woodhead: *Metal Science*, 1976, vol. 10, 3, pp. 105-12.
28. J. Wadsworth, J. H. Woodhead, and S. R. Keown: *Metal Science*, 1976, vol. 10, 10, pp. 342-48.
29. J. Wadsworth: *Metall. Trans. A*, 1983, vol. 14A, pp. 285-94.
30. Sekine, Inoue, and Ogasawara: *Trans. I. S. I. Japan*, 1968, vol. 8, p. 101.
31. K. Narita: *Trans. I. S. I. Japan*, 1975, vol. 27, p. 145.
32. S. Koyama, T. Ishii, and K. Narita: *J. Japan Inst. Metals*, 1973, vol. 37, p. 191.
33. W. Roberts and A. Sandberg: Swedish Institute for Metals Report IM-1489, October 1980.
34. B. W. Christ and G. V. Smith: *Acta Metall.*, 1967, vol. 15, pp. 809-16.
35. F. B. Pickering and T. Gladman: Metallurgical Developments in Carbon Steels, I. S. I. London, 1963, vol. 10.
36. F. B. Pickering: *Physical Metallurgy and the Design of Steels*, Applied Science Publishers, London, 1978.
37. A. Melander: *Scand. J. of Metallurgy*, 1978, vol. 7, pp. 109-13.
38. K. Hanson and J. W. Morris Jr.: *J. Appl. Phys.*, 1975, vol. 46, 983, pp. 2378-82.
39. D. J. Bacon, U. F. Kocks, and R. O. Scattergood: *Phil. Mag.*, 1973, vol. 28, pp. 1241-63.
40. R. Ebeling and M. F. Ashby: *Phil. Mag.*, 1966, vol. 13, pp. 805-34.
41. M. F. Ashby and R. Ebeling: *Trans. AIME*, 1966, vol. 236, pp. 1396-1404.
42. T. Gladman, D. Dulieu, and I. D. McIvor: *Microalloying 75*, M. Korchinsky, ed., Union Carbide Corp., New York, NY, 1976, vol. 1, pp. 32-55.
43. U. F. Kocks: *Phil. Mag.*, 1966, vol. 13, pp. 541-66.
44. K. J. Irvine, F. B. Pickering, and T. Gladman: *J. I. S. I.*, 1967, vol. 207, pp. 161-82.
45. E. Smith: *Acta Metall.*, 1966, vol. 14, pp. 583-93.